NANO MICRO

small

Cell Adhesion

Synthetic cell–cell adhesion with high stability and robustness is demonstrated by S. H. Yun and co-workers using a bioorthogonal click chemistry-based cell gluing method. On page 6458, they show how tetrazine (Tz) and trans-cyclooctene (TCO) conjugated to the cell surface form covalent bonds between cells within 10 min in aqueous conditions. Glued cells remain viable and stably attached in blood flow, showing the potential for biomedical applications.

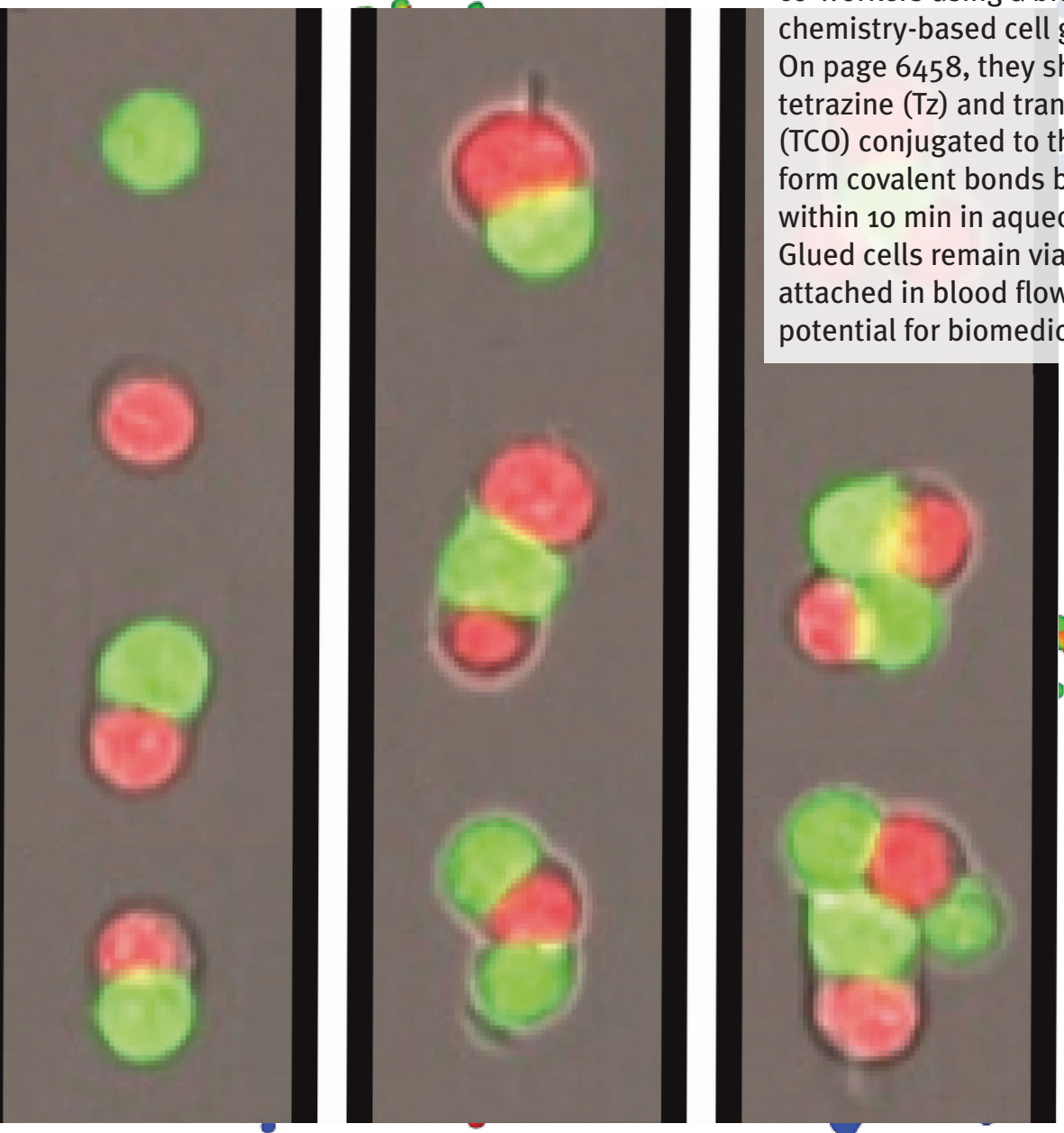

48/2015

WILEY-VCH

Bioorthogonal Click Chemistry-Based Synthetic Cell Glue
S. H. Yun and co-workers

www.MaterialsViews.com

Bioorthogonal Click Chemistry-Based Synthetic Cell Glue

*Heebeom Koo, Myunghwan Choi, Eunha Kim, Sei Kwang Hahn, Ralph Weissleder, and Seok Hyun Yun**

Artificial methods of cell adhesion can be effective in building functional cell complexes in vitro, but methods for in vivo use are currently lacking. Here, a chemical cell glue based on bioorthogonal click chemistry with high stability and robustness is introduced. Tetrazine (Tz) and trans-cyclooctene (TCO) conjugated to the cell surface form covalent bonds between cells within 10 min in aqueous conditions. Glued, homogeneous, or heterogeneous cell pairs remain viable and stably attached in a microfluidic flow channel at a shear stress of 20 dyn cm^{-2}. Upon intravenous injection of assembled Jurkat T cells into live mice, fluorescence microscopy shows the trafficking of cell pairs in circulation and their infiltration into lung tissues. These results demonstrate the promising potential of chemically glued cell pairs for various applications ranging from delivering therapeutic cells to studying cell–cell interactions in vivo.

1. Introduction

Close contact between cells is essential to establish intercellular communication, exert collective functions, and form multicellular structures.[1] In nature, the contact interaction is typically achieved by a series of surface adhesion molecules and connections.[2] A synthetic method to control the contact and binding between cells would be useful in tissue engineering and cell therapy[3] by producing functional cell pairs and higher complexes.[4] A promising approach for artificial cell adhesion is to modify cell surfaces with high-affinity "glue" molecules. This has been demonstrated by using complementary nucleotide sequences,[4a,5] avidin–biotin interaction,[6] antibody dimers,[7] and aptamers.[8] The complementary macromolecules can provide binding specificity for bottom-up assembly of multicellular, multidimensional units in vitro. A drawback of these noncovalent methods is their limited tensile strength and stability, particularly for in vivo use, which can be degraded by enzymes, such as proteases, DNases, and RNases.[8] In comparison, covalent chemical bonds using bioorthogonal small molecules (<1 kDa) offer compelling advantages. First, the chemical bonds are irreversible and therefore more stable and robust than biological bonds. Second, small chemicals can be introduced to the cell surface at higher density,[9] which can yield stronger, multivalent adhesion between cells. Furthermore, the cost for synthesis and storage can be considerably lower for chemicals than proteins and nucleotides. Recently, chemical binding of cells has been demonstrated by using oxime-hydroquinone chemistry, but this method required a long binding time of over 1 h due to its slow reaction rate.[10]

Here, we introduce click chemistry for stable and robust cell gluing. Click chemistry has originally been referred to chemical reactions with high yield, simple

Dr. H. Koo, Prof. M. Choi, Prof. S. H. Yun
Wellman Center for Photomedicine
Massachusetts General Hospital
and Harvard Medical School
65 Landsdowne St., UP-5, Cambridge, MA 02139, USA
E-mail: syun@hms.harvard.edu
Prof. M. Choi
Department of Global Biomedical Engineering
Center for Neuroscience and Imaging Research
Sungkyunkwan University
Institute for Basic Science
Suwon, Gyeong Gi-Do 440-746, South Korea
Prof. E. Kim, Prof. R. Weissleder
Center for Systems Biology
Massachusetts General Hospital and Harvard Medical School
Boston, MA 02114, USA
Prof. E. Kim
Department of Molecular Science and Technology
Ajou University
Suwon 443-749, South Korea
Prof. S. K. Hahn
Department of Materials Science and Engineering
Pohang University of Science and Technology
Kyungbuk 790–784, South Korea

DOI: 10.1002/smll.201502972

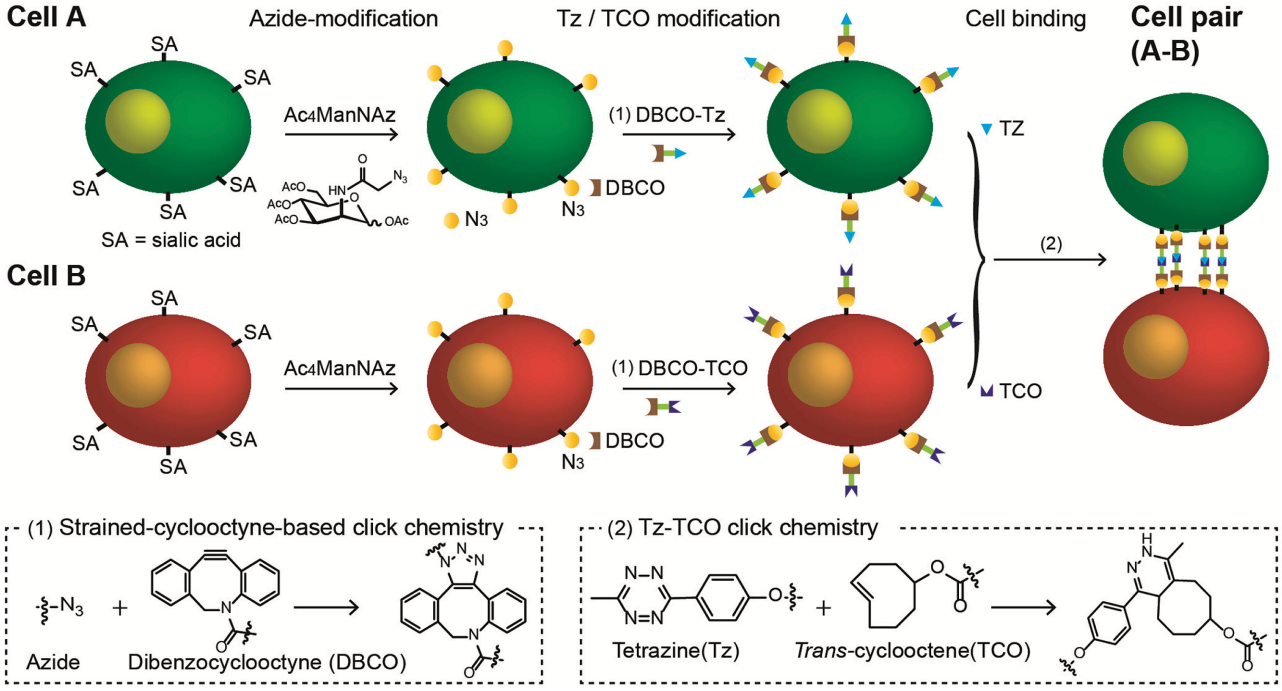

Scheme 1. Illustration of the cellular gluing method based on metabolic glycoengineering and double click chemistry.

reaction condition, and inoffensive by-products.[11] Cycloaddition reaction between azide (N_3) and alkyne groups with copper catalysts has been widely used. To date, several click chemistry reactions including strained alkynes/azide and tetrazine (Tz)/*trans*-cyclooctene (TCO) have been developed, which occur in aqueous conditions without using toxic copper catalyst.[12] The "copper-free" click chemistry has been widely used to attach individual molecules and nanoparticles for molecular assay,[13] targeted imaging,[14] and drug delivery.[15] Beyond attaching small molecules and nanoparticles, gluing macroscopic objects,[16] such as biological cells, pose significant challenge that requires more stringent optimizations in terms of the reaction rate and binding force, as well as biocompatibility. In this work, we have used a double click chemistry strategy for efficient and robust cell–cell gluing. Prior to attaching Tz and TCO molecules, cells have been modified first by metabolic glycoengineering, introducing azide groups onto the cell surface with minimal biological perturbations (**Scheme 1**).[17] Tz and TCO are then attached to the azide using azide-dibenzocyclootyne (DBCO) click chemistry via heterobifunctional crosslinkers, Tz–DBCO and TCO–DBCO (Figure S1, Supporting Information).[18] When mixed together, the Tz- and TCO-modified cells form a pair (Scheme 1). We have performed cell-binding force measurements and animal injection study to assess the potential of chemically glued cells for in vivo applications.

2. Results and Discussion

2.1. Gluing Cells by Metabolic Glycoengineering and Double Click Chemistry

We used four human and mouse cell lines—namely A549 human lung cancer cells, human Jurkat T lymphocytes, NIH3T3 murine fibroblasts, and EL4 murine lymphoma cells. Cell viability after azide modification showed a marked drop at concentrations of tetraacetylated *N*-azidoacetyl-*d*-mannosamine ($Ac_4ManNAz$) higher than 60×10^{-6} M (Figure S2a, Supporting Information). In all experiments otherwise stated, we used a nontoxic concentration of 50×10^{-6} M. The subsequent treatment with Tz–DBCO or TCO–DBCO had little effect on cell viability at concentrations up to 100×10^{-6} M (Figure S2b,c, Supporting Information). Fluorescence microscopy performed after conjugating Cy3 to the azide group in situ by administrating Cy3-DBCO showed the spatially uniform, high expression of the azide groups in A549 cells (Figure S3, Supporting information). Tz–Cy3 and TCO–Cy3 conjugates (Figure S4, Supporting Information) were used to measure the overall amount of TCO and Tz molecules on the cell surface (Figures S5–S8, Supporting Information). Among the four cell lines, Jurkat T and A549 cells had significantly higher incorporation than NIH3T3 cells, and EL4 cells showed the lowest incorporation (**Figure 1**a). The cell line-dependent incorporation of Tz and TCO was consistent with the known difference in the amount of sialic acids on the cell surface.[19]

2.2. Viability, IL-2 Secretion, and Migration of Glued Cells

We next investigated the viability of Jurkat T and A549 cells as glued pairs. A549 adhesion cells were grown on a microfluidic chamber in monolayer and modified with Tz as above. Jurkat T cells were modified with TCO and added on top of the Tz-modified A549 cell layer (Figure 1b). After 10 min of incubation for Tz–TCO reaction, Jurkat T cells were glued on to A549 cells. The glued cells showed no dissociation under the flow at a rate of 1 mL min^{-1} (Figure 1c). By contrast,

www.MaterialsViews.com

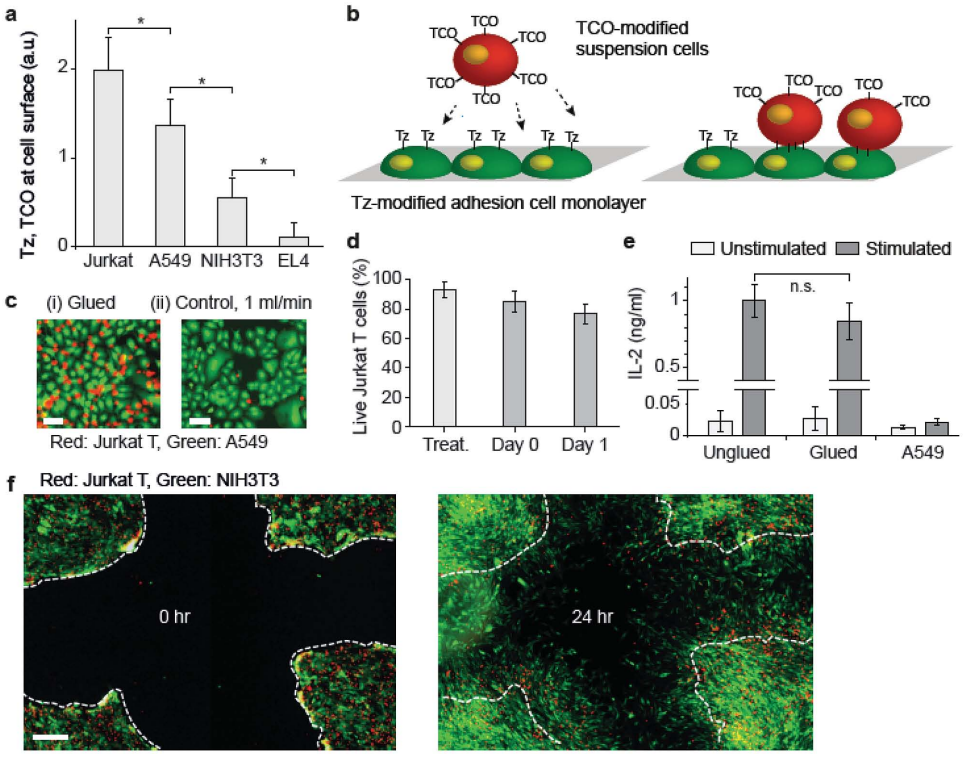

Figure 1. Analysis of viability and function of glued cells. a) Measured amount of Tz and TCO groups on cell surface after chemical modification for four different cell lines. Error bars, s.d.; *, *t*-test $P < 0.005$ (sample $n = 10$). b) Illustration of cellular gluing between suspension (red) and adhesion (green) cells. c) Fluorescence images of the glued cells in a microfluidic chamber after washing with a flow at 1 mL mm^{-1}. Scale bar, 50 μm. d) Viability of Jurkat–Jurkat glued cells measured by using calcein AM/ethidium homodimer 1 assay after incubation for 1 d in culture. e) IL-2 secretion from glued Jurkat T cells. Error bars, s.d. (sample $n = 5$). f) Microscopic images showing the migration of NIH3T3 cells (green) carrying Jurkat T cells (red) glued on their surface. Scale bar, 100 μm.

nonmodified Jurkat T cells in control experiments were almost completely washed away in same condition (Figure 1c and Figure S9, Supporting Information). Live/dead cell assays using calcein AM and ethidium homodimer 1 showed that 93% of Jurkat T cells were alive within 1 h after TCO modification. 85% of Jurkat T cells were alive at 1 h after gluing to A549 cells, and 77% remained viable after further incubation in cell media for 24 h (Figure 1d). Jurkat T cells secret interleukin-2 (IL-2) when stimulated by lectins. To test whether this intrinsic function is preserved after gluing, we administered 10 μg mL^{-1} phytohemaglutinin to Jurkat T glued on A549 cells and, after 1 d of incubation, measured the amount of secreted IL-2 by human IL-2 enzyme-linked immuno assay (ELISA). IL-2 secretion from Jurkat T cells was slightly, but insignificantly, decreased in the glued cells compared to unmodified cells (Figure 1e). The slight decrease in IL-2 secretion may originate from that their surface was partially covered by A549 cells, but the result indicates that the intrinsic function was largely unaffected.

We also investigated the migration function of NIH3T3 fibroblasts after gluing with Jurkat T cells grown on culture wells. After gluing, a cross scratch pattern was created for wound-healing assay. After incubation for 1 d, NIH3T3 cells were found to have migrated into the scratched area (Figure 1f). A significant fraction of the migrated NIH3T3 cells had one or two Jurkat T cells associated with them. This result not only shows the mobility of glued cell pairs but also suggests the potential of a cell delivery strategy by gluing a cargo cell to a mobile carrier cell.

2.3. Microfluidic Measurement of the Binding Force between Glued Cells

To measure the binding force between glued cells, we used flow-induced shear in the microfluidic channel (5 mm in width and 0.8 mm in height) and measured the number of suspension cells attached on adhesion cells (**Figure 2**a). TCO-modified Jurkat T cells glued onto Tz-modified A549 cells remained attached after applying flow for 1 min at flow rates up to 60 mL min^{-1}, the maximum available tested (Figure 2b). Similar results were obtained for Jurkat T cells glued on NIH3T3 cells (Figure S10, Supporting Information). The shear stress exerted on the cells was calculated to be about 20 dyn cm^{-2} (2 Pa) at 60 mL min^{-1}.[20] The ratios of the remaining Jurkat T cells to A549 cells were 1.05 at 10 min after gluing and 0.75 after incubation for 24 h in full growth medium containing serum (Figure 2c). The ratio was 0.61 at Day 2, indicating that more than half of the glued cells remained bound to A549 cells (Figure S11, Supporting Information). Similar ratios, 1.0 at Day 0 and 0.65 at Day 1, were measured for Jurkat T and NIH3T3 cells, respectively (Figure 2d). The ratios were significantly lower for EL4 cells compared to Jurkat T (0.18 per A549 cell) (Figure S12,

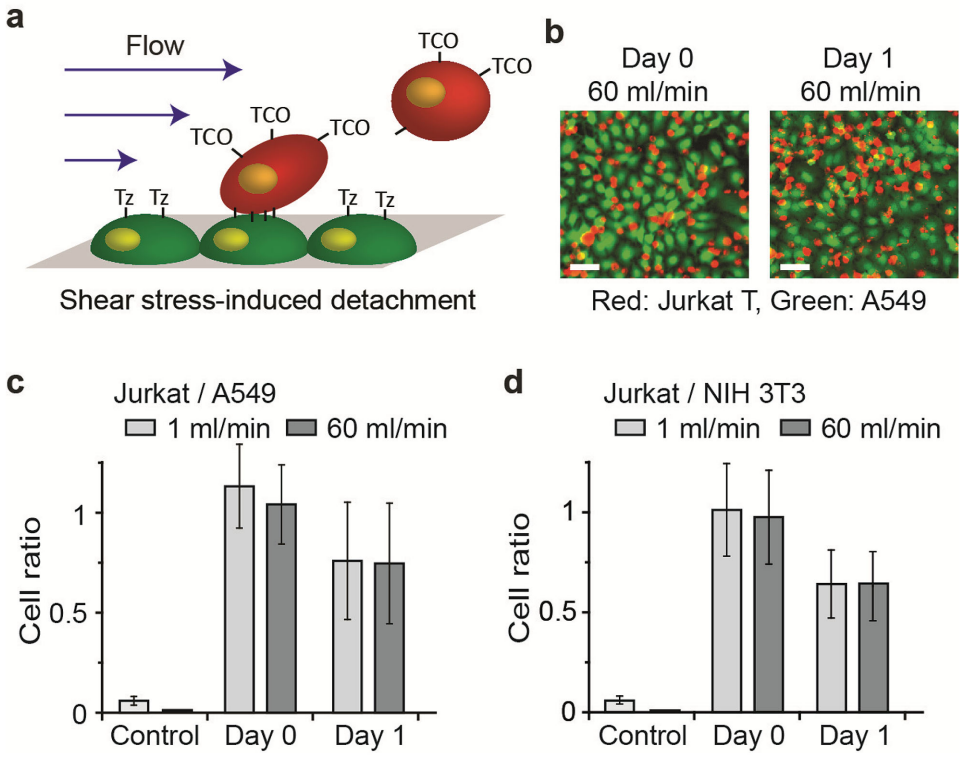

Figure 2. Analysis of the binding force between glued cells. a) Illustration of the flowing test on the glued cells in microfluidic chambers. b) Fluorescence images of the glued Jurkat T cells on A549 cells. Scale bar, 50 μm. Flow at 60 mL min^{-1} was applied for duration of 1 min, at 10 min (day 0), and 24 h (day 1) after Tz–TCO gluing. The ratio of cell numbers in the glue pairs after flow for c) Jurkat–A549 and d) Jurkat–NIH3T3 cells.

Supporting Information). The lowest ratio of 0.07 was obtained with EL4 on NIH3T3 cells. These results are consistent with the measured amount of Tz and TCO molecules for those cell types (Figure 1a). The more Tz and TCO groups are available on the cell surface, the more cell pairs are produced, resulting in the greater binding force.

2.4. Shape and Bonding Efficiency of Glued Cells

When three groups comprising unmodified control (Hoechst, blue), Tz-modified (CellTracker red), and TCO-modified (CellTracker green) Jurkat T cells were incubated on a nutating mixer for 10 min, only Tz- and TCO-modified cells were specifically bound (**Figure 3**a). Tz- and TCO-modified cells in suspension culture produced not only two-cell pairs (doublet) but also triplets and other multicellular clusters comprising three or more cells of opposite click molecules (Figure 3b). Scanning electron microscope (SEM) images revealed a rather close adhesion between cells (Figure 3c). The contact area was 10%–15% of the entire cell surface area. Flow cytometry allowed quantitative analysis of the glued cells in large population (≈1 million). In controls, only 0.1% cells were double positive, confirming the low rates of nonclick attachment events (Figure 3d). The double-positive population was 5.4% when the cells were modified with Tz– and TCO–DBCO at 10×10^{-6} M. At our protocol concentration of 50×10^{-6} M, about 46% of the Tz- and TCO-modified cells formed two- or multiple-cell pairs. Increasing the concentration to 100×10^{-6} M did not much improve the glued cell population.

We compared our protocol with an alternative bonding method based on azide-DBCO click chemistry (Figure S13, Supporting Information).[21] The azide-DBCO click chemistry has a reaction rate of $k_2 = 0.31$ M^{-1} s^{-1}, substantially lower than the typical Tz–TCO reaction rate[22] of $k_2 = 820$ M^{-1} s^{-1}. Azide-modified Jurkat T cells were treated with homobifunctional crosslinker, DBCO–polyethyleneglycol$_4$–DBCO, at a concentration of 50×10^{-6} M to produce DBCO-modified cells and these cells were mixed with pristine azide-modified cells. The ratio of the glued cells after incubation for 10 min was measured to be only 4.1% (Figure 3e), much lower than 46% for the Tz–TCO method. Increasing the incubation time did not improve the gluing ratio of azide-DBCO chemistry. Efficiencies of 5.6% and 7.1% were measured with incubation times of 1 and 2 h, respectively (Figure S14, Supporting Information). To analyze the amount of azide, DBCO, Tz, and TCO on A549 cells, we treated the cells with DBCO–Cy3, azide–Cy3, TCO–Cy3, and Tz–Cy3, respectively, and measured the Cy3 fluorescence intensity by using microscopy. The measurements showed that the amounts of DBCO and azide were not much different from those of Tz and TCO (Figure S15, Supporting Information). Therefore, we attributed the low gluing efficiency of the control DBCO-modified cells mainly to the low reaction rate of azide-DBCO click chemistry. This result represents the critical role of rapid Tz–TCO click reaction for gluing cells.

www.MaterialsViews.com

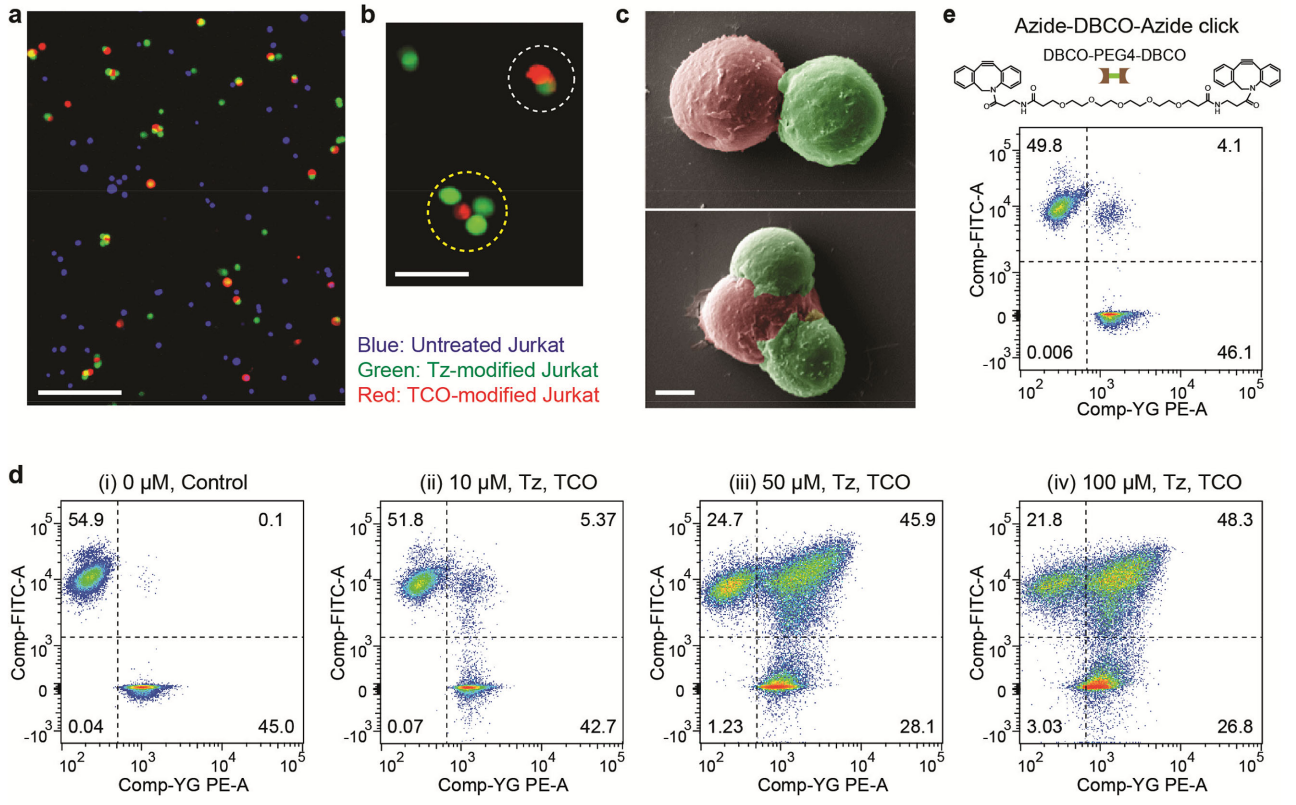

Figure 3. Microscopy and cytometry analyses. a) Fluorescence images of glued Jurkat T cells in suspension. Scale bar, 100 μm. b) High-resolution image of two-cell doublet and four-cell quartet glued cells (circles). Scale bar, 50 μm. c) SEM images of doublet (top) and triplet (bottom) glued Jurkat T cells (pseudocolored green and red). Scale bar, 5 μm. Flow cytometry data of Jurkat T cells glued with different concentrations of d) Tz and TCO or e) by azide-DBCO click chemistry. Inset, a schematic of DBCO–PEG_4–DBCO.

2.5. High-Throughput Imaging Cytometry Analysis of Cell Complexes

To analyze the individual population of glued cell groups, we used an imaging cytometry system (**Figure 4**a), which generates high-speed microscopic images of cells during flow cytometry analysis (Figure 4b). From over 7000 images of cell groups, the numbers of cells in singlet, doublet, triplet, quartet, and multiple groups ($N > 4$) were counted (Figure 4c,d). We found 29% of the Jurkat T cells remained as singlet, and 43% of cells were in doublet (Figure 4e). Since there are two cells in each doublet, the ratio of doublet to singlet is 0.74 (=21.5/29). 11% of the cells were in triplet, which make the triplet to single ratio to be 0.13 (=3.7/29). These results indicate that the current protocol is optimized for producing doublets with high yield. Increasing cell concentration during incubation tended to generate more higher-order cell complexes. Forward and side light-scattering analysis showed reduced aspect ratios (deviation from spherical shapes) and increased scattering area of the glued-cell samples compared to controls, as expected from their shapes (Figure S13, Supporting Information). The specific ratios of glued cells vary depending on the amount of the Tz or TCO molecules at the cell surface. For EL4 cells, the total ratio of the glued cells was about 19%, and 80% of which were in doublet (Figure 4f). The relatively low yield of glued cells for EL4 cells is due to the low amount of sialic acid on the cell surface.

2.6. Glued Cells Injected into Blood Circulation In Vivo

To investigate the in vivo stability of glue cells, we injected two-color glued, Jurkat T cells (Hoechst and CellTracker green) into wild-type mice (c57BL/6 strain) by retro-orbital injection while visualizing blood vessels in the intact ear skin by the laser-scanning two-photon excitation fluorescence microscopy.[23] Video-rate imaging showed doublet glued cells flowing in the blood vessels, both veins and arteries, within a field of view (**Figure 5**a). Rapid sequestration of injected cells in the lung capillary beds is well known.[24] Three-color Jurkat T cells, including Hoechst-stained unmodified controls (blue), in equal population (≈10^6 total) were injected intravenously into wild-type mice; and after 20 min, the lung tissues were harvested and imaged ex vivo under the two-photon fluorescence microscope. A large number of cells, including single cells, doublet, and higher-order complexes, were found in the lung tissue (Figure 5b). Most of them were trapped within lung capillary beds.[24] About 31% of cells made in contact with other cells consisted of red and green cells (Figure 5c). This ratio was consistent with the population statistics measured in vitro (Figure 4b) and at least

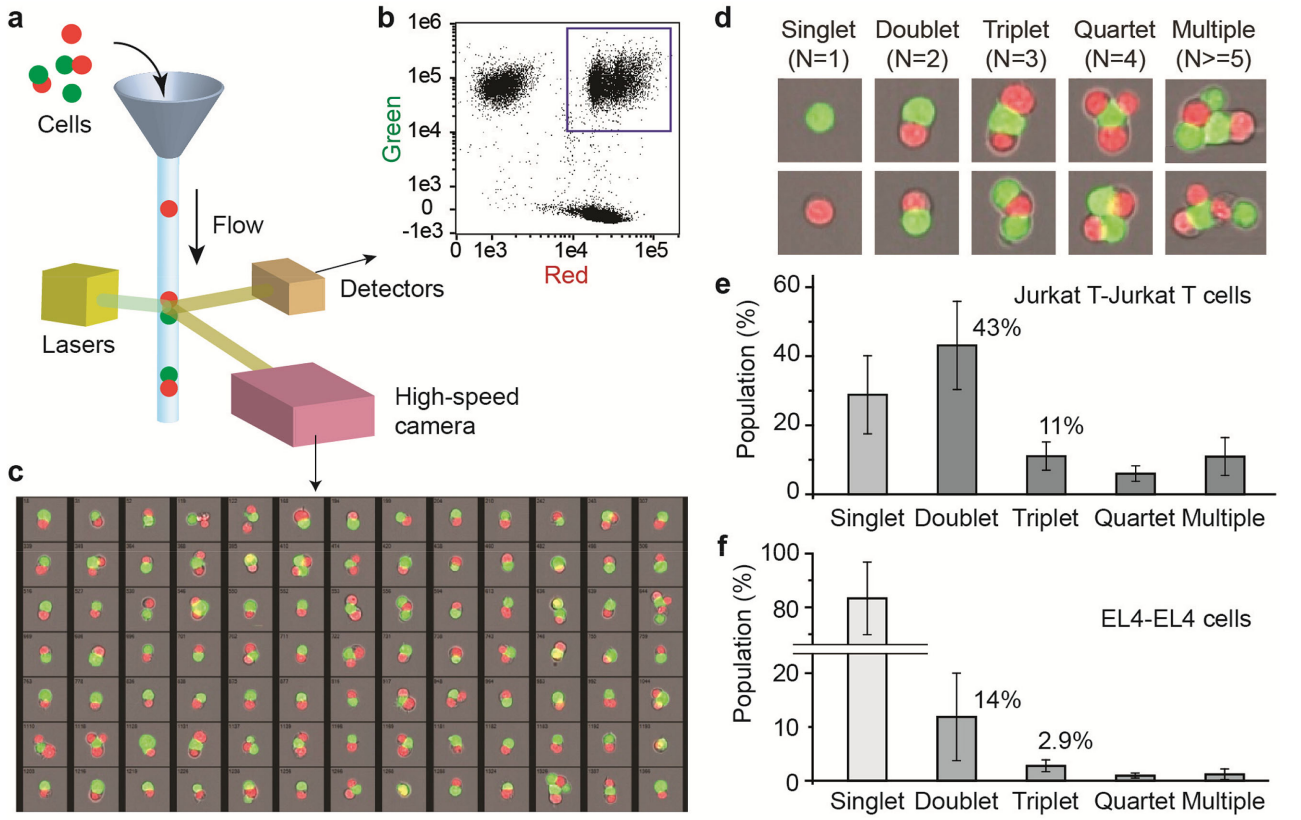

Figure 4. Analysis of glued cells by imaging cytometry. a) Illustration showing simultaneous flow cytometry and microscopic imaging. b) Measured cytometry graph. The population in the box corresponds to glued cells. c) Cytometry images showing glued population of green- and red-labeled Jurkat T cells after focus filtering. d) Representative captured images of various cell groups. e) The measured statistics of various cell groups for the case of Jurkat–Jurkat cells. f) Statistics for EL4–EL4 cells.

sixfold higher than nonspecific pairs in contact (Figure 5c). These results show that the majority of glued cells remain attached in the tissue.

3. Conclusion

We have demonstrated a cell gluing method based on metabolic glycoengineering and double click chemistry. The metabolically introduced azide groups covalently link the click molecules to the cell surface without using biological links, such as antibodies, establishing "all-chemical" binding between cells. Our comparison study between Tz–TCO with azide-DBCO highlights the importance of the fast reaction rate for gluing cells, which allows multivalent bonds to be formed within a finite time of cell–cell contact during incubation. The chemically glued cells are alive and stably bound after 1 d incubation in vitro, and able to withstand a shear stress over 20 dyn cm^{-2}, which is higher than typical vessel-wall shear stress levels of 1–6 dyn cm^{-2} in veins and 15 dyn cm^{-2} in arteries.[25] The glue strength and the output yield of cell pairs depend on the cell type and increase with to the amount of click molecules on the cell surfaces. Most tumor cell lines overexpress sialic acids.[26] Other strategies, such as amide coupling or lipid insertion, could be also used to introduce Tz or TCO groups onto the cell surface. Intravenously injected cell pairs were found in the blood stream and traffic to various organs including the lung. Delivering cell pairs to other target tissues, such as inflammation sites or tumors, should be possible when specialized homing cells including stem cells or leukocytes are glued as carriers.[3b,27] Our study represents the first demonstration of injection and imaging of glued cells in vivo. The click chemistry-based cell glue with high specificity, fast reaction rate, stability, and biocompatibility is promising for the development of a wide range of biomedical applications in vivo. Furthermore, the gluing technology demonstrated here may be applied to the adhesion of any cell types onto artificial surfaces treated with click molecules for broad applications in cell-based sciences and engineering.[28]

4. Experimental Section

Materials: Tetrazine–dibenzo cyclootyne (Tz–DBCO), *trans*-cyclooctene–polyethyleneglycol$_{12}$–dibenzo cyclootyne (TCO–DBCO), *trans*-cyclooctene–amine (TCO–amine), and Cy3–tetrazine (Cy3–Tz) were purchased from Click Chemistry Tools (Scottsdale, AZ, USA). Cy3–NHS ester was purchased from Lumiprobe (FL, USA). Tetraacetylated *N*-azidoacetyl-*d*-mannosamine (Ac_4ManNAz), CellTracker green CMFDA, CellTracker red CMTPX, CellTracker blue CMAC, Hoechst 33342, Prestoblue cell viability reagent, calcein AM, and ethidium homodimer 1, RPMI 1640, DMEM, fetal bovine serum (FBS), and antibiotic–antimycotics were purchased from Life

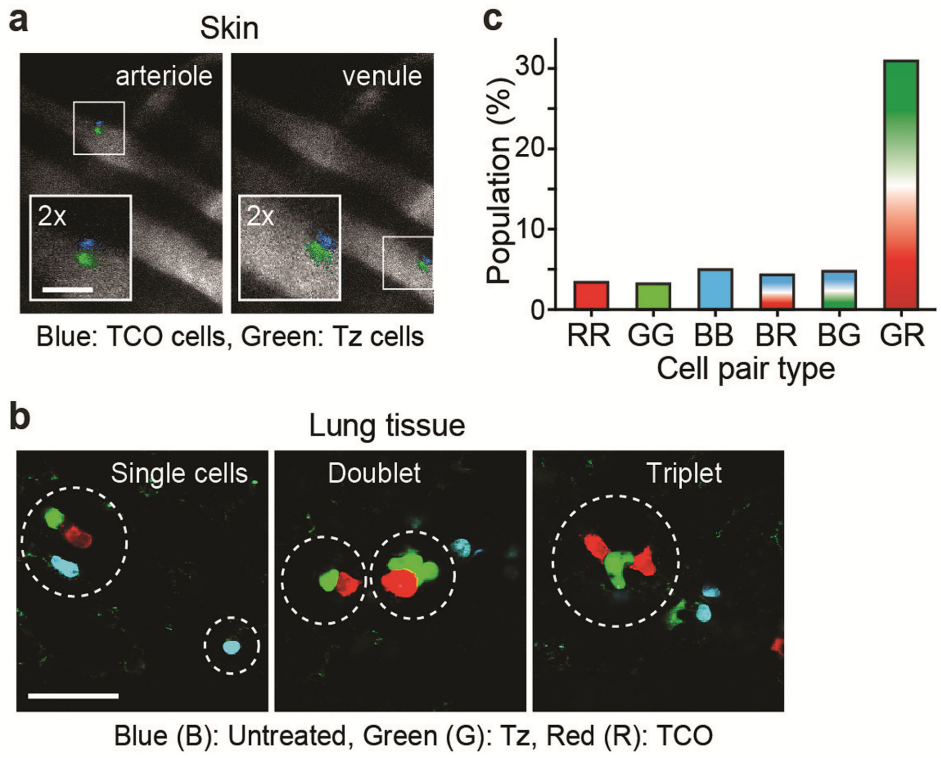

Figure 5. Cells injected into mice. a) Intravital images of glued Jurkat T cells flowing in the blood vessels of the ear skin. Scale bar, 100 μm. b) Fluorescence images of Jurkat T cells in lung tissues harvested about 20 min after injection. Scale bar, 100 μm. c) Measured population of cells in contact in the lung tissues. R, G, and B represent the color of cell: 'GR' indicates cell pairs consisting of Tz-modified (green) and TCO-modified (red) cells.

technologies (Grand Island, NY, USA). μ-Slide I 0.8 Luer microfluidic chamber was purchased from ibidi GmbH (Munich, Germany). 70 kDa rhodamine–dextran was purchased from Sigma-Aldrich (St. Louis, MO, USA). All chemicals were of analytical grade and used without further purification.

Synthesis of Cy3–TCO: A solution of TCO–Amine HCl salt (2.0 mg, 0.0075 mmol) and TEA (5 μL, 0.036 mmol) in DMF (100 μL) was incubated at room temperature for 5 min. To a reaction mixture, Cy3–NHS ester (5 mg, 0.0068 mmol) solution in DMF (200 μL) was added. Reaction mixture was stirred at ambient temperature for 1 h. Desired compound was purified by using standard HPLC techniques performed on a Waters' (Milford, MA, USA) liquid chromatography-mass spectrometry (LC-MS) system. For preparative runs, an Atlantis Prep T3 OBDTM 5 μ M column was used (eluents 0.1% TFA (v/v) in water and MeCN; gradient: 0–1.5 min, 5%–100% B; 1.5–2.0 min 100% B). The title compound was purified in 62.5% yield and its identity was confirmed by LC-MS. For LC-ESI-MS analyses, a Waters XTerra C18 5 μm column was used.

Cell Culture: A549 (Human lung adenocarcinoma), Jurkat T (clone E6–1, human T lymphocyte), NIH3T3 (mouse fibroblast), and EL4 cells (mouse T lymphocyte) were purchased from ATCC (Manassas, VA, USA). A549 and Jurkat T cells were maintained in RPMI1640 medium containing 10% FBS and 1% antibiotic–antimycotics in humidified 5% CO_2 atmosphere at 37 °C. DMEM instead of RPMI1640 was used for NIH3T3 and EL4 cells. For fluorescence labeling, cells were stained with CellTracker green CMFDA, CellTracker red CMTPX, or CellTracker blue CMAC for 30 min in serum-free media.

Imaging of Tz or TCO Groups on the Cell Surface: Cells were washed with PBS and incubated with 5×10^{-6} M Cy3–TCO or Cy3–Tz and 5×10^{-6} M Hoechst 33342 in serum-free media for 10 min. After washing with PBS, the cells were observed by a microscope (IX51, Olympus, Chelmsford, MA, USA). The intensity of Cy3 fluorescence was analyzed by using ImageJ.

Cell Gluing: Cells were grown in full growth media containing 50×10^{-6} M Ac_4ManNAz for 3 d and treated with 50×10^{-6} M Tz–DBCO or TCO–DBCO for 30 min in PBS containing Ca^{2+} and Mg^{2+}. After washing with PBS, the cells were collected and mixed together at 5×10^5 cells mL^{-1} concentration and incubated for 10 min on a nutating mixer (Labnet, NJ, USA).

Cell Viability Test: 2×10^3 A549 or NIH3T3 cells were seeded on 96-well plates. After 1 d, the cells were treated with Ac_4ManNAz and Tz–DBCO or TCO–DBCO, as described above. The cells were then incubated in 90 μL serum-free media with 10 μL Prestoblue solution for 2 h. Then, the fluorescence intensity from the wells was measured at 560-nm excitation and 590-nm emission by using a GEMINI EM microplate reader (Molecular Devices, CA, USA) and its ratio to that from untreated controls determined the cell viability. For calcein AM/ethidium homodimer 1 assay, Jurkat T Cells were stained by CellTracker blue CMAC before treatment of TCO–DBCO and gluing. After gluing, they were incubated in serum-free medium containing 2×10^{-6} M calcein AM and 4×10^{-6} M ethidium homodimer 1 for 30 min, and incubated in serum-free medium for 15 min. After washing with PBS, the sample was observed by a microscope (IX51, Olympus, Chelmsford, MA, USA).

Interleukin-2 (IL-2) ELISA: 2×10^4 Tz-modified A549 cells on 96-well plates were incubated with 5×10^4 TCO-modified Jurkat T cells for 10 min. After washing away unglued cells with PBS, and remaining cells were stimulated with 10 μg mL^{-1} phytohemaglutinin and 1 ng mL^{-1} phorbol 12-myristate 13-acetate. After 1 d, supernatants were harvested and the amounts of IL-2 were analyzed by human IL-2 ELISA kit (Thermo Scientific, Rochester, USA).

Fluidic Chamber Study: 2×10^3 A549 or NIH3T3 cells in 200 μL full growth medium were seeded and grown on a μ-Slide I 0.8 Luer fluidic chamber and incubated with Ac_4ManNAz and with Tz–DBCO as described above. Then, they were incubated for 10 min with 1×10^4 TCO-modified or control bare Jurkat T cells in 200 μL serum-free RPMI1640 containing 1% w/v BSA on nutating mixer. While applying predetermined flow rates by using a syringe pump, the cells were observed with a microscope (IX51, Olympus, Chelmsford, MA, USA). The number of the cells per field of view (200 μm × 200 μm) was counted.

Cell Migration Test: 2×10^5 Tz-modified NIH3T3 cells and 5×10^5 TCO-modified Jurkat T cells were incubated in a 24-well plate for 10 min. After washing away unglued cells, the center of each well was scratched by using the tip of a 100 μL pipet in a crisscross pattern. The images were obtained by using a microscope (IX51, Olympus, Chelmsford, MA, USA).

SEM Imaging: Glued cells were loaded on circular cover glass and stored in ethanol, dried by critical point dryer 931 GL (tousimis, MD, USA), and coated with 5 nm Au by a 300T dual head sputter coater (EMS, PA, USA). The samples were imaged by Evo 55 environmental SEM (Zeiss, Oberkochen, Germany).

Flow Cytometry Analysis: The glued cells were transferred to a 5 mL polystyrene round-bottom tube with cell-strainer cap (mesh size: 30 μm, BD bioscience, CT, USA) for filtering and analyzed by a FACSAria cell sorting system (BD bioscience, CT, USA) or an Amnis ImageStreamX Mark II imaging flow cytometer (Amnis Corporation, WA, USA).

Intravital Imaging: All animal experiments were performed in compliance with institutional guidelines and approved by the subcommittee on research animal care at the Harvard Medical School. All experiments used 7- to 14-week-old C57BL/6J mice (Jackson Laboratory). 70-kDa rhodamine-dextran (100 μL of 3% w/v) was intravenously administered to visualize blood vessels. While imaging the blood vessels in the ear skin of an anesthetized mouse, blood vessels were imaged under a home-built two-photon microscope; glued Jurkat T cells stained with Hoechst 33342 and CellTracker green were administered intravenously (100 μL, 5×10^6 cells mL^{-1}). Movies of the flowing cells were captured at 30 Hz for duration of 5 min following the injection. For ex vivo imaging, anesthetized mice were injected intravenously with glued cells stained with CellTracker red and CellTracker green (100 μL, 5×10^5 cells mL^{-1}). Twenty minutes after injection, the mice were killed, and the lung tissues were harvested, cut into 5 mm × 5 mm slices, put on slide glass, and observed under the two-photon microscope.

Two-Photon Microscopy: We used a home-built, video-rate, two-photon microscope. The system equipped a mode-locked Ti-Sapphire laser (MaiTai DeepSee eHP, Newport) as an excitation source, which provides ≈120 fs width pulses at 80 MHz repetition rate. The scanning unit is composed of a polygon mirror for fast axis (x) and a galvanometer mirror for slow axis (y), allowing a frame rate of 30 Hz. A 20× 1.0-NA water-immersion objective lens (Olympus) was used for all experiments. The emitted light was detected by three photomultiplier tubes through dichroic and bandpass filters for the blue channel (330–480 nm), green channel (500–550 nm), and red channel (560–670 nm).

Supporting Information

Supporting Information is available from the Wiley Online Library or from the author.

Acknowledgements

The authors thank Danny Cao and Scott Mordecai for their help in cytometry. This work was supported in part by the US National Science Foundation (ECCS-1264356), Department of Defense (FA9550–11–1–0331), and Mid-career Researcher Program through the National Research Foundation of Korea (2012R1A2A2A06045773), National IT Industry Promotion Agency (IT Consilience Creative Program, NIPA-2014-H0201–14–1001), and the Medical Discovery Postdoctoral Fellowship Award from MGH.

[1] a) R. Ahrends, A. Ota, K. M. Kovary, T. Kudo, B. O. Park, M. N. Teruel, *Science* **2014**, *344*, 1384; b) A. S. Meshel, Q. Wei, R. S. Adelstein, M. P. Sheetz, *Nat. Cell Biol.* **2005**, *7*, 157.

[2] a) S. Lee, J. Mandic, K. J. Van Vliet, *Proc. Natl Acad. Sci.* **2007**, *104*, 9609; b) N. Aceto, A. Bardia, D. T. Miyamoto, M. C. Donaldson, B. S. Wittner, J. A. Spencer, M. Yu, A. Pely, A. Engstrom, H. L. Zhu, B. W. Brannigan, R. Kapur, S. L. Stott, T. Shioda, S. Ramaswamy, D. T. Ting, C. P. Lin, M. Toner, D. A. Haber, S. Maheswaran, *Cell* **2014**, *158*, 1110.

[3] a) K. Ohashi, T. Yokoyama, M. Yamato, H. Kuge, H. Kanehiro, M. Tsutsumi, T. Amanuma, H. Iwata, J. Yang, T. Okano, Y. Nakajima, *Nat. Med.* **2007**, *13*, 880; b) J. M. Karp, G. S. Leng Teo, *Cell Stem Cell* **2009**, *4*, 206.

[4] a) Z. J. Gartner, C. R. Bertozzi, *Proc. Natl Acad. Sci.* **2009**, *106*, 4606; b) M. E. Todhunter, N. Y. Jee, A. J. Hughes, M. C. Coyle, A. Cerchiari, J. Farlow, J. C. Garbe, M. A. LaBarge, T. A. Desai, Z. J. Gartner, *Nat. Meth.* **2015**, *12*, 975.

[5] K. Vogel, M. Glettenberg, H. Schroeder, C. M. Niemeyer, *Small* **2013**, *9*, 255.

[6] B. Wang, J. Song, H. Yuan, C. Nie, F. Lv, L. Liu, S. Wang, *Adv. Mater.* **2014**, *26*, 2371.

[7] C. H. Kim, J. Y. Axup, A. Dubrovska, S. A. Kazane, B. A. Hutchins, E. D. Wold, V. V. Smider, P. G. Schultz, *J. Am. Chem. Soc.* **2012**, *134*, 9918.

[8] X. Xiong, H. Liu, Z. Zhao, M. B. Altman, D. Lopez-Colon, C. J. Yang, L.-J. Chang, C. Liu, W. Tan, *Angew. Chem., Int. Ed.* **2013**, *52*, 1472.

[9] J. B. Haun, N. K. Devaraj, S. A. Hilderbrand, H. Lee, R. Weissleder, *Nat. Nano* **2010**, *5*, 660.

[10] D. Dutta, A. Pulsipher, W. Luo, M. N. Yousaf, *J. Am. Chem. Soc.* **2011**, *133*, 8704.

[11] H. C. Kolb, M. G. Finn, K. B. Sharpless, *Angew. Chem., Int. Ed.* **2001**, *40*, 2004.

[12] J. C. Jewett, C. R. Bertozzi, *Chem. Soc. Rev.* **2010**, *39*, 1272.

[13] a) M. Shelbourne, X. Chen, T. Brown, A. H. El-Sagheer, *Chem. Commun.* **2011**, *47*, 6257; b) K. Wang, A. Sachdeva, D. J. Cox, N. W. Wilf, K. Lang, S. Wallace, R. A. Mehl, J. W. Chin, *Nat. Chem.*

2014, *6*, 393; c) J. A. Prescher, C. R. Bertozzi, *Cell* **2006**, *126*, 851; d) V. M. Peterson, C. M. Castro, H. Lee, R. Weissleder, *ACS Nano* **2012**, *6*, 3506; e) M. Colombo, S. Sommaruga, S. Mazzucchelli, L. Polito, P. Verderio, P. Galeffi, F. Corsi, P. Tortora, D. Prosperi, *Angew. Chem., Int. Ed.* **2012**, *51*, 496; f) W. Xi, T. F. Scott, C. J. Kloxin, C. N. Bowman, *Adv. Funct. Mater.* **2014**, *24*, 2572.

[14] a) R. Rossin, P. Renart Verkerk, S. M. van den Bosch, R. C. M. Vulders, I. Verel, J. Lub, M. S. Robillard, *Angew. Chem., Int. Ed.* **2010**, *49*, 3375; b) S. T. Laughlin, J. M. Baskin, S. L. Amacher, C. R. Bertozzi, *Science* **2008**, *320*, 664.

[15] H. Koo, S. Lee, J. H. Na, S. H. Kim, S. K. Hahn, K. Choi, I. C. Kwon, S. Y. Jeong, K. Kim, *Angew. Chem., Int. Ed.* **2012**, *51*, 11836.

[16] A. Harada, R. Kobayashi, Y. Takashima, A. Hashidzume, H. Yamaguchi, *Nat. Chem.* **2011**, *3*, 34.

[17] E. Saxon, C. R. Bertozzi, *Science* **2000**, *287*, 2007.

[18] A. A. Neves, H. Stöckmann, Y. A. Wainman, J. C. H. Kuo, S. Fawcett, F. J. Leeper, K. M. Brindle, *Bioconj. Chem.* **2013**, *24*, 934.

[19] Y. Guo, E. Rumschlag-Booms, J. Wang, H. Xiao, J. Yu, J. Wang, L. Guo, G. Gao, Y. Cao, M. Caffrey, L. Rong, *Virol. J.* **2009**, *6*, 39.

[20] J. Park, Z. Fan, C. X. Deng, *J. Biomech.* **2011**, *44*, 164.

[21] a) M. F. Debets, S. S. van Berkel, J. Dommerholt, A. J. Dirks, F. P. J. T. Rutjes, F. L. van Delft, *Acc. Chem. Res.* **2011**, *44*, 805; b) N. K. Devaraj, R. Weissleder, *Acc. Chem. Res.* **2011**, *44*, 816.

[22] M. R. Karver, R. Weissleder, S. A. Hilderbrand, *Bioconj. Chem.* **2011**, *22*, 2263.

[23] D. Sarkar, J. A. Spencer, J. A. Phillips, W. Zhao, S. Schafer, D. P. Spelke, L. J. Mortensen, J. P. Ruiz, P. K. Vemula, R. Sridharan, S. Kumar, R. Karnik, C. P. Lin, J. M. Karp, *Blood* **2011**, *118*, e184.

[24] a) M. J. Mitchell, E. Wayne, K. Rana, C. B. Schaffer, M. R. King, *Proc. Natl Acad. Sci. USA* **2014**, *111*, 930; b) T. Maldiney, A. Bessière, J. Seguin, E. Teston, S. K. Sharma, B. Viana, A. J. J. Bos, P. Dorenbos, M. Bessodes, D. Gourier, D. Scherman, C. Richard, *Nat. Mater.* **2014**, *13*, 418.

[25] J. M. Barnes, J. T. Nauseef, M. D. Henry, *PLoS One* **2012**, *7*, e50973.

[26] A. Matsumoto, N. Sato, K. Kataoka, Y. Miyahara, *J. Am. Chem. Soc.* **2009**, *131*, 12022.

[27] P. Teriete, S. Banerji, M. Noble, C. D. Blundell, A. J. Wright, A. R. Pickford, E. Lowe, D. J. Mahoney, M. I. Tammi, J. D. Kahmann, I. D. Campbell, A. J. Day, D. G. Jackson, *Mol. Cell* **2004**, *13*, 483.

[28] a) X. Yao, R. Peng, J. Ding, *Adv. Mater.* **2013**, *25*, 5257; b) F. Yang, C. G. Williams, D.-A. Wang, H. Lee, P. N. Manson, J. Elisseeff, *Biomaterials* **2005**, *26*, 5991.

Received: September 30, 2015
Published online: November 19, 2015